

Electronic Supplementary Information

Trisiloxane-centred Metal-Organic Frameworks and Hydrogen Bonded Assemblies

Luke C. Delmas,^a Andrew J. P. White,^a David Pugh,^a Peter N. Horton,^b Simon J. Coles,^b Paul D. Lickiss^a and Robert P. Davies^{*a}

^aDepartment of Chemistry, Imperial College London, South Kensington, London, UK SW7 2AZ.

^bEPSRC National Crystallography Service, Chemistry, University of Southampton, Highfield, Southampton SO17 1BJ, UK

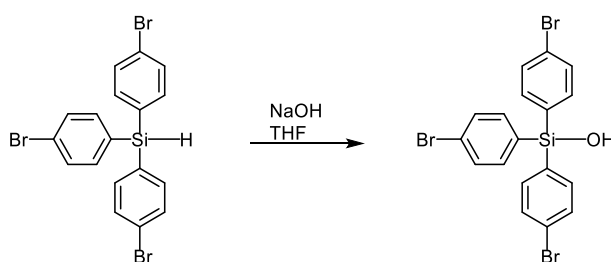
*E-mail: r.davies@imperial.ac.uk; Tel: +44 (0)207 5945754

General Methods:

NMR spectra were recorded on a Bruker 400 MHz (^1H) spectrometer and all chemical shifts are reported in δ (ppm) using the relevant residual solvent peaks as internal standards.¹ Mass spectra were recorded using a Waters LCT Premier (ESI) spectrometer. Powder X-ray diffraction (PXRD) studies were performed using a Panalytical MPD X-ray diffractometer with $\text{Cu-K}\alpha$ (1.54 Å) radiation. Thermogravimetric analysis was carried out under a nitrogen atmosphere using a Mettler Toledo instrument under a constant stream of dry nitrogen gas (flow rate 50 mL min^{-1}) over the temperature range 30–800 °C and at a heating rate of 5 °C min^{-1} . X-ray data was collected using a Rigaku FRE+ (**IMP-20**), Rigaku 007HF (**IMP-21**) or Agilent Xcalibur PX Ultra (**L-H₆**) diffractometer. Solutions were solved and refined using SHELX and SHELXTL,^{2, 3} as well as Olex-2,⁴ and WinGX.⁵ The SQUEEZE routine within PLATON was used to remove heavily disordered solvents from the **IMP-21** structure.⁶ Graphics were generated using CrystalMaker.⁷ A summary of the crystallographic data is presented in Table S1.

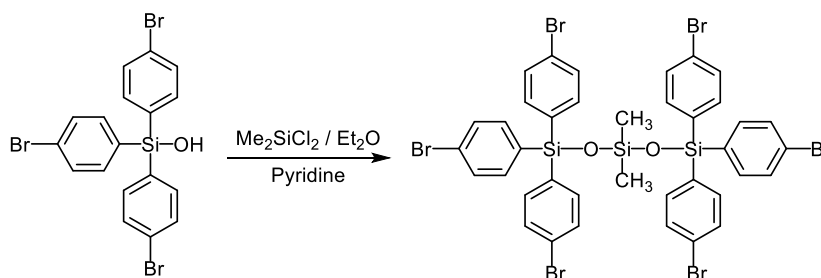
Synthesis:

Tris(4-bromophenyl)silanol



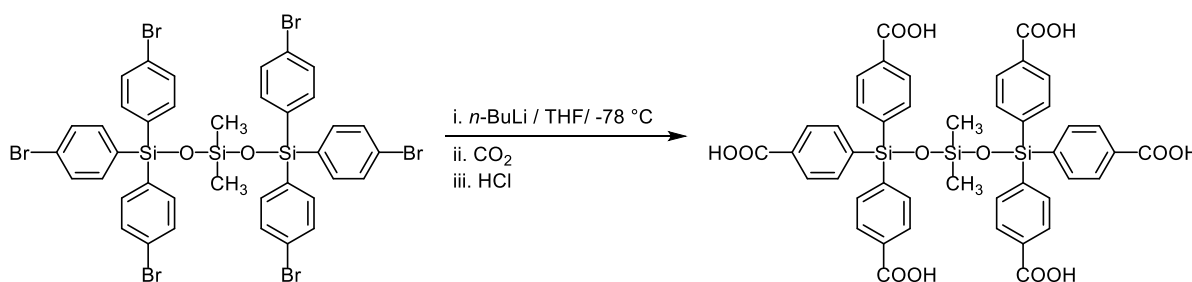
Tris(4-bromophenyl)silane⁸ (1.0 g, 2.0 mmol) was dissolved in THF (10 mL) and the resulting solution treated with 4 M aqueous NaOH (0.60 mL, 2.4 mmol). The mixture was stirred overnight and subsequently concentrated to approximately 2 mL after which chloroform (20 mL) and 1 M aqueous HCl (10 mL) was added. The organic phase was separated, dried (MgSO_4) and evaporated to afford a colourless oil. This oil was taken up into hot hexanes (5 mL) and allowed to stand. Tris(4-bromophenyl)silanol crystallised as colourless needles and was collected by suction filtration: 0.71 g (70 %). M.p. 125 - 127 °C; ^1H NMR (400 MHz, CDCl_3) δ = 7.54 (d, 6H, J = 8.33 Hz, Ar-H), 7.43 (d, 6H, J = 8.33 Hz, Ar-H); $^{13}\text{C}\{^1\text{H}\}$ NMR (100 MHz, CDCl_3) δ = 136.5, 133.0, 131.5, 125.9; ^{29}Si NMR (80 MHz, CDCl_3) δ = -12.6; MS (ESI-): calcd (monoisotopic) for $\text{C}_{18}\text{H}_{12}\text{Br}_3\text{OSi}$ m/z = 508.8208; found m/z = 508.8225 [$\text{M} - \text{H}$]⁻; Br_3 isotope pattern; IR (ATR): ν (cm^{-1}) = 3169 (br, O-H), 1573, 1478, 1377, 1118, 1066, 1009, 836, 803, 733, 536, 515.

1,1,1,5,5,5-hexakis(4-bromophenyl)-3,3-dimethyltrisiloxane



Tris(4-bromophenyl)silanol (1.0 g, 2.0 mmol) was taken up in diethyl ether (15 mL) and dry pyridine (0.50 mL, 6.2 mmol) was added to the solution which was then stirred for 5 minutes at ambient temperature. The reaction vessel was placed in an ice-water bath and Me_2SiCl_2 (0.12 mL, 0.97 mmol) was added dropwise. This mixture was left to stir for approximately 12 hours, slowly warming to ambient temperature. The reaction was quenched with 1 M aqueous HCl (10 mL) and washed with diethyl ether (2×15 mL). The organic fractions were dried (MgSO_4) and concentrated to afford a colourless oil which was purified by column chromatography (8 hexanes : 1 EtOAc). 1,1,1,5,5,5-hexakis(4-bromophenyl)-3,3-dimethyltrisiloxane was collected as a white fluffy solid: 0.45 g, 42%. M.p. 48-51 °C; ^1H NMR (400 MHz, CDCl_3) δ = 7.43 (d, 12H, J = 8.29 Hz, Ar-H), 7.22 (d, 12H, J = 8.29 Hz, Ar-H), 0.07 (s, 6H, Si- CH_3); $^{13}\text{C}\{^1\text{H}\}$ NMR (100 MHz, CD_3Cl) δ = 136.4, 133.2, 131.4, 125.7, 1.67; ^{29}Si NMR (80 MHz, CDCl_3) δ = -20.7 (Ar_3Si), -16.45 (Me_2Si); IR (ATR): ν (cm^{-1}) = 1571, 1480, 1377, 1260 (Si- CH_3), 1185, 1116, 1086, 1065 (Si-O), 1045, 1009, 841, 808, 734.

1,1,1,5,5,5-hexakis(4-carboxyphenyl)-3,3-dimethyltrisiloxane ($L\text{-H}_6$)



1,1,1,5,5,5-hexakis(4-carboxyphenyl)-3,3-dimethyltrisiloxane was synthesized following a modified procedure by Davies and co-workers.⁹ A 2.5 M solution of *n*-butyllithium in hexanes (2.2 mL, 5.5 mmol) was added to a flask containing anhydrous THF (35 mL) under a nitrogen atmosphere immersed in a dry ice-acetone bath. A solution of 1,1,1,5,5,5-hexakis(4-bromophenyl)-3,3-dimethyltrisiloxane (1.0 g, 0.92 mmol) in THF (20 mL) was then slowly added to the vessel and the mixture left to stir for 2 hours. Carbon dioxide was subsequently bubbled through the reaction mixture for 3 hours after which the mixture was left to stir overnight, gradually warming to ambient temperature. The reaction was quenched with 1 M aqueous hydrochloric acid (15 mL) and the organic phase was separated and evaporated to

a sticky residue. Hot EtOAc (20 mL) was added to the mixture with vigorous stirring resulting in a white suspension being formed. The title compound was isolated as a white powdery solid after suction filtration: 0.36 g (45 %). M.p., decomposed above 290 °C; Anal. calcd. for $C_{44}H_{36}O_{14}Si_3$: C, 60.54; H, 4.16. Found: C, 60.35; H, 4.21. 1H NMR (400 MHz, DMSO- D_6) δ (ppm) = 13.1 (s, 6H, COOH), 7.88 (d, 12H, J = 8.29 Hz, Ar-H), 7.52 (d, 12H, J = 8.29 Hz, Ar-H), 0.09 (s, 6H, Si- CH_3); $^{13}C\{^1H\}$ NMR (100 MHz, $CDCl_3$) δ (ppm) = 167.0, 139.1, 134.6, 132.6, 128.6, 1.21; ^{29}Si NMR (80 Hz, $CDCl_3$) δ (ppm) = -22.31 (Ar_3Si), -15.12 ($Si(CH_3)_2$); MS (ESI-): calcd (monoisotopic) for $C_{44}H_{35}O_{14}Si_3$ m/z = 871.1329; found m/z = 871.1324 [$M - H$] $^-$; IR (ATR): ν (cm^{-1}) = 2965 (C-H), 2868 (O-H), 2665, 2542, 1729, 1684, 1602, 1555, 1500, 1419, 1390, 1317, 1286, 1261 (Si- CH_3), 1223, 1181, 1099, 1084, 1098, 1047 (Si-O-Si), 1017, 848, 839, 801, 760.

[Mn₃(L)(DMF)₄].6DMF (IMP-20)

L-H₆ (10 mg, 12 μ mol) and Mn(OAc)₂.4H₂O (0.017 g, 69 μ mol) were combined in a glass vial to which DMF (2.8 mL) and acetic acid (280 μ l) were added. The mixture was sonicated until all reagents had dissolved. The vial was sealed and slowly heated in an oven to 120 °C over 3 hours, held at 120 °C for 42 hours and cooled gradually to room temperature over 3 hours. Colourless crystals were collected by suction filtration which were washed with fresh DMF (3 \times 5 mL) and air dried. Yield = 18 mg (86 % based on L-H₆). IR (ATR): ν (cm^{-1}) = 1650, 1582, 1533, 1496, 1386, 1256, 1104, 1036, 1014, 858, 798, 774, 724, 704. Attempts to prepare an activated sample of the MOF for further sorption studies were unsuccessful due to decomposition of the MOF (as evidenced by PXRD studies).

[Zn₃(L)(OAc)][Me₂NH₂].3.75DMF (IMP-21)

L-H₆ (10 mg, 12 μ mol) and Zn(OAc)₂ (0.013 g, 69 μ mol) were combined in a glass vial to which DMF (2.8 mL) and acetic acid (300 μ l) were added. The mixture was sonicated until all reagents had dissolved. The vial was sealed and slowly heated in an oven to 120 °C over 3 hours, held at 120 °C for 42 hours and cooled gradually to room temperature over 3 hours. Colourless crystals were collected by suction filtration which were washed with fresh DMF (3 \times 5 mL) and air dried. Yield = 13 mg (76 % based on L-H₆) IR (ATR): ν (cm^{-1}) = 1655, 1601, 1542, 1498, 1389, 1261, 1105, 1044, 1017, 842, 799, 772, 727, 705. Attempts to prepare an activated sample of the MOF for further sorption studies were unsuccessful due to decomposition of the MOF (as evidenced by PXRD studies).

Crystallography Notes:

The ligand $\text{L-H}_6\text{-AcOH}\cdot\frac{1}{2}\text{H}_2\text{O}$ was refined as a 2-component twin (twin law -1 0 0 0 -1 0.0 0.5 0 1). The water molecule was positionally disordered over two sites, as well as a symmetry operation, hence it was modelled with varying occupancy which refined to ~58 and 42 %. No protons attached to the water molecule could be found from the difference map and, owing to the multiple hydrogen bonding interactions involving the disordered water, protons were not added using calculated values. This created problems when trying to use HTAB to add these hydrogen bonds to the CIF. Therefore the PLAT430_ALERT_2_B alerts do reflect genuine hydrogen bonds, but the uncertainty regarding the position of the hydrogen atoms means that they are not included in the CIF. It also means that the reported moiety formula and sum lines differ from the calculated values by 2H per asymmetric unit.

For **IMP-20**, there is positional disorder of multiple DMF molecules (both bound and free). Despite this, all the DMF molecules were successfully modelled even though various geometrical (SAME, FREE, BUMP) and displacement (DELU, SIMU, RIGU) restraints were employed.

All seven of the unique carboxylic acid groups in the structure of **IMP-21** are involved in bonding to metal atoms. As such it is reasonable to assume that they are all deprotonated, and so contribute a -7 charge. The three zinc atoms contribute $+6$ (though there are four unique sites occupied by zinc centres, two of these (Zn1 and Zn4), are special positions and so only count as 50% in the asymmetric unit) and so there is a "missing" positive charge. The most likely explanation was the presence of a dimethylammonium cation in the disordered solvent region which could not be explicitly located.

The included solvent was found to be highly disordered, and the best approach to handling this diffuse electron density was found to be the SQUEEZE routine of PLATON.⁵ This suggested a total of 1439 electrons per unit cell, equivalent to 179.9 electrons per asymmetric unit. Deducting the electron density of the presumed cation in this region ($\text{C}_2\text{H}_8\text{N}$, 27 electrons) leaves 152.9 electrons per asymmetric unit due to the solvent. The solvent was not clearly identifiable hence the reaction solvent DMF ($\text{C}_3\text{H}_7\text{NO}$, 40 electrons) was assumed. 3.75 DMF molecules corresponds to 150 electrons, so this was used. As a result, the atom list for the asymmetric unit is low by $\text{C}_2\text{H}_8\text{N} + 3.75(\text{C}_3\text{H}_7\text{NO}) = \text{C}_{13.25}\text{H}_{34.25}\text{N}_{4.75}\text{O}_{3.75}$ (and that for the unit cell low by $\text{C}_{106}\text{H}_{274}\text{N}_{38}\text{O}_{30}$) compared to what is actually presumed to be present.

The central, Si1-based, SiMe_2 moiety was found to be disordered. Two orientations were identified of ~86 and 14% occupancy, their geometries were optimised, the thermal parameters of adjacent atoms were restrained to be similar, and only the non-hydrogen atoms of the major occupancy orientation were refined anisotropically (those of the minor occupancy orientation were refined isotropically).

L-H₆ H-bonded Network

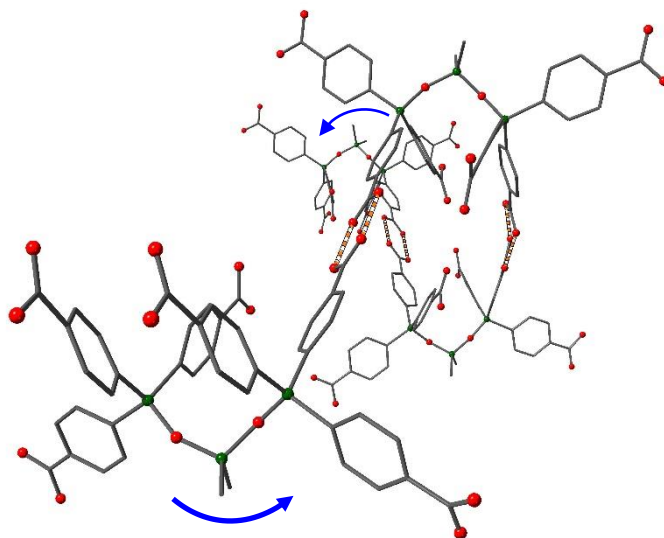


Figure S1: Arrangement of L-H₆ molecules leading to formation of a single coiled array. Blue arrows indicated overall handedness of coil. Colour scheme: O, red; C, grey; Si, green.

Several interactions between the 3 individual coiled arrays (shown in Figure S1) hold the tightly knit molecular bundle together. In the first interaction (Figure S2 A), a pendant COOH group (O13 & O14) of an adjacent coiled array approaches a COOH dimer (O7 & O8) of a neighbouring strand perpendicularly where only one of the oxygen atoms (O13) donates a hydrogen bond to O7 of the dimer.

The second interaction (Figure S2 B) is more complex: this 6-component interaction involves two neighbouring pendant COOH groups (O23 & O24) from a single strand and a single pendant COOH group (O19 & O20) each from the other two strands that make up the molecular bundle. These all come together via hydrogen bonding to two 'bridging' water molecules (O33).

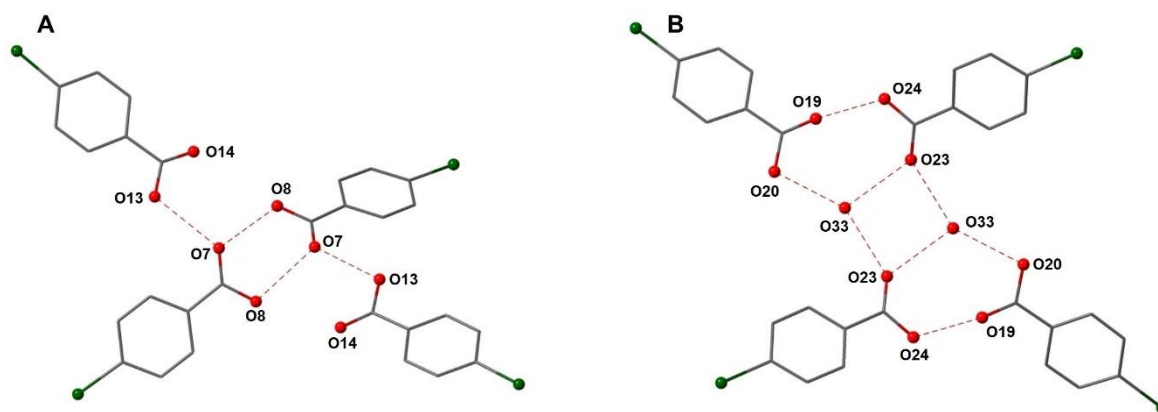


Figure S2: Hydrogen bonding interactions between coiled arrays of L-H₆ molecules. Colour scheme: O, red; C, grey; Si, green.

These 2D corrugated layers assemble closely in the b-direction to effect satisfactory packing in the crystal lattice as shown in Figure S3.

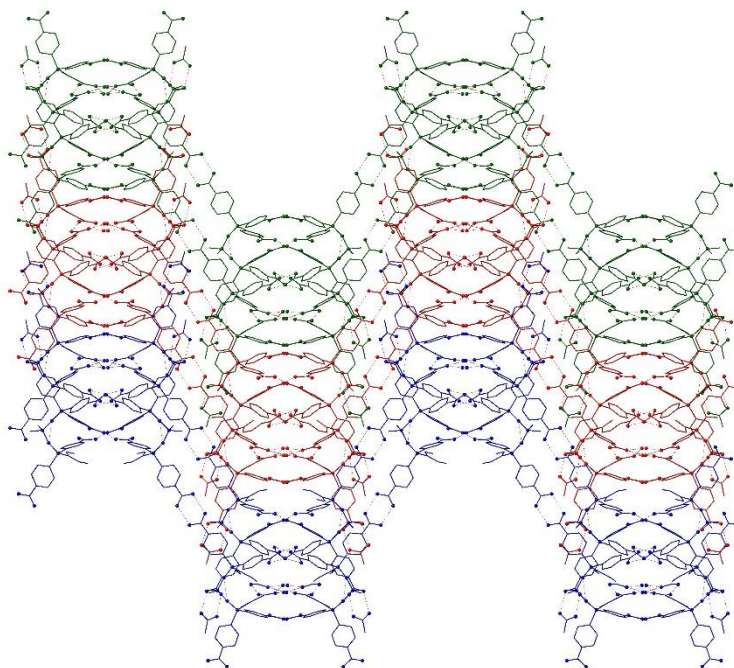


Figure S3: Three separate 2D corrugated layers (shown in green, red and blue) in the structure of L-H₆ acetic acid solvate

IMP-20 MOF Network

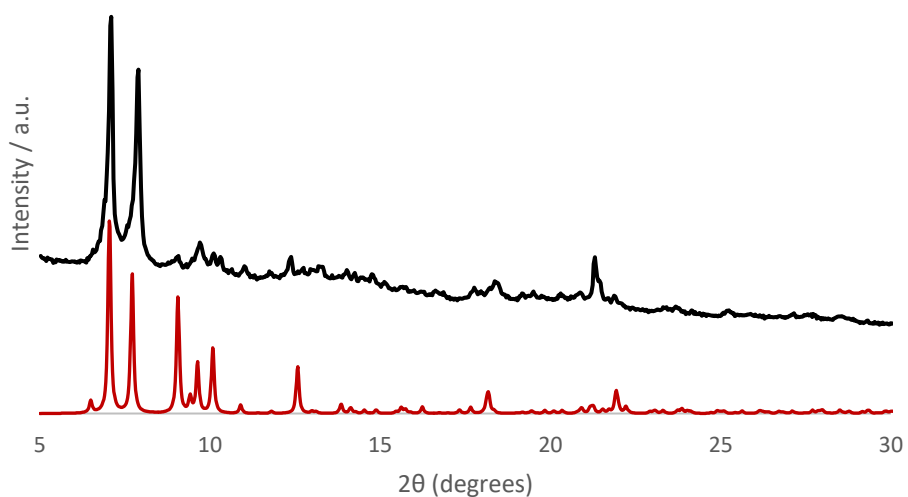


Figure S4: Overlaid PXRD diffractograms for **IMP-20**. Simulated (bottom) and as-synthesised material (top).

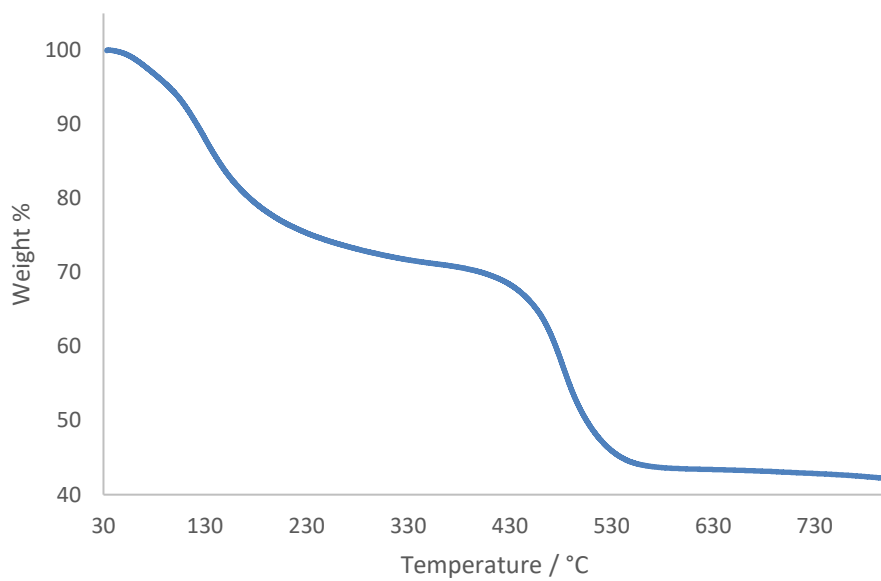


Figure S5: TGA trace for **IMP-20**

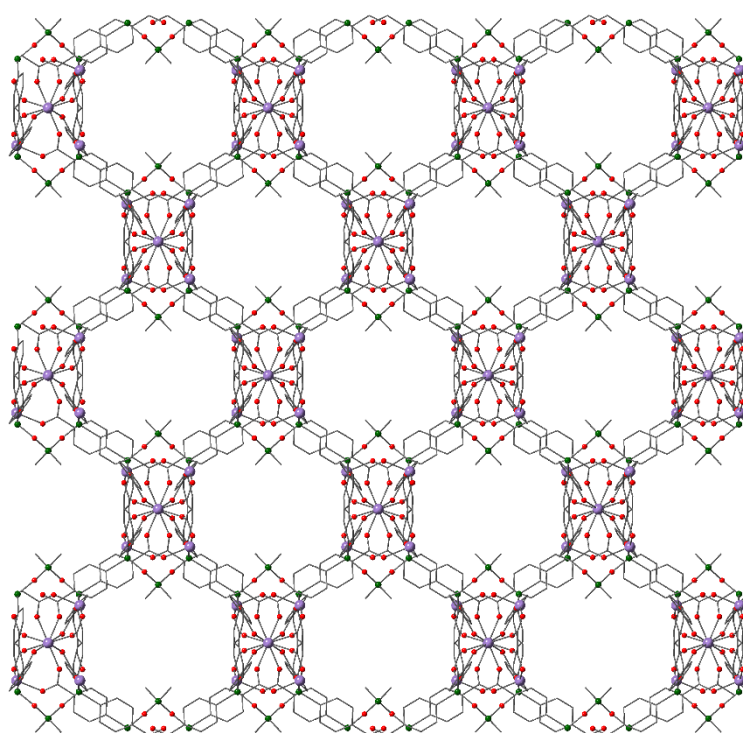


Figure S6: View of a portion of the **IMP-20** network along the [101] direction. Disorder, solvent molecules and hydrogen atoms omitted for clarity. Colour scheme: Mn, purple; O, red; C, grey; Si, green.

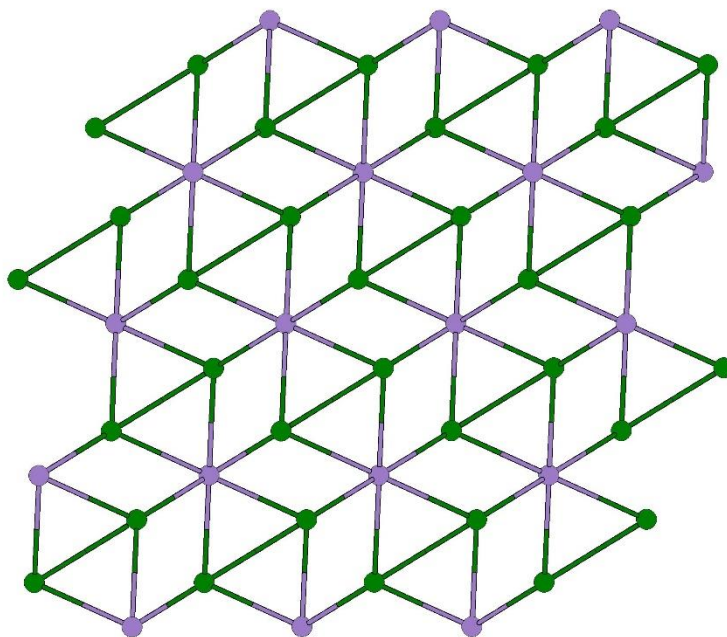


Figure S7: Topological view of **IMP-20** when **L** is considered as two conjoined tetrahedral nodes (shown in green) and Mn nodes as 6-connected (shown in purple). Structure has been optimised using Systre¹⁰ such that the ideal symmetry of the crystal net has been assumed. This topology [whose point symbol is $\{3^2.4^2.5.6\}_2\{3^2.4^2.5^2.8^7.9.10\}$] has not been previously reported to the best of our knowledge.

IMP-21 MOF Network

Charge Balance Discussion

The asymmetric unit of **IMP-21** was found to contain one molecule of **L** (6-), one acetate anion (1-), and three Zn(II) cations leading to a net negative charge of 1-. There are numerous examples of anionic MOFs in the literature where charge balance is achieved by the presence of disordered dimethylammonium cations (formed by the hydrolysis of DMF under solvothermal conditions) in the pores of the MOF.¹¹⁻¹⁴ This prompted us to record the ¹H NMR spectrum of a digested sample of IMP-21 crystals. A strong smell of dimethylamine (formed by deprotonation of Me₂NH₂⁺ once the MOF has collapsed) was observed on mixing approximately 5 mg IMP-21 with an 8 wt% NaOD solution in D₂O. Additionally, a peak attributable to dimethylamine was clearly visible at 1.75 ppm in the ¹H NMR spectrum providing further evidence for the presence of Me₂NH₂⁺ ions in the pores of the MOF.

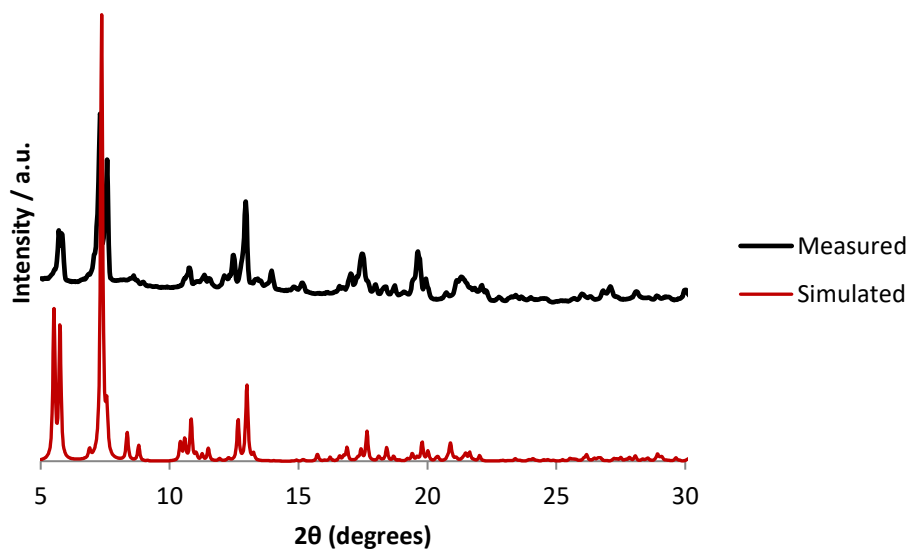


Figure S8: Overlaid PXRD diffractograms for **IMP-21**: Simulated (bottom) and as-synthesised material (top).

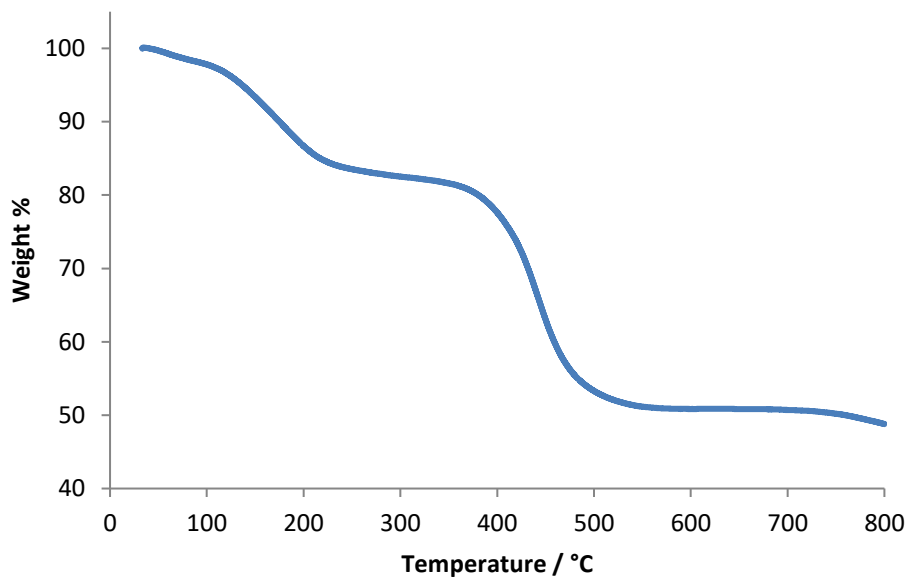


Figure S9: TGA trace for **IMP-21**

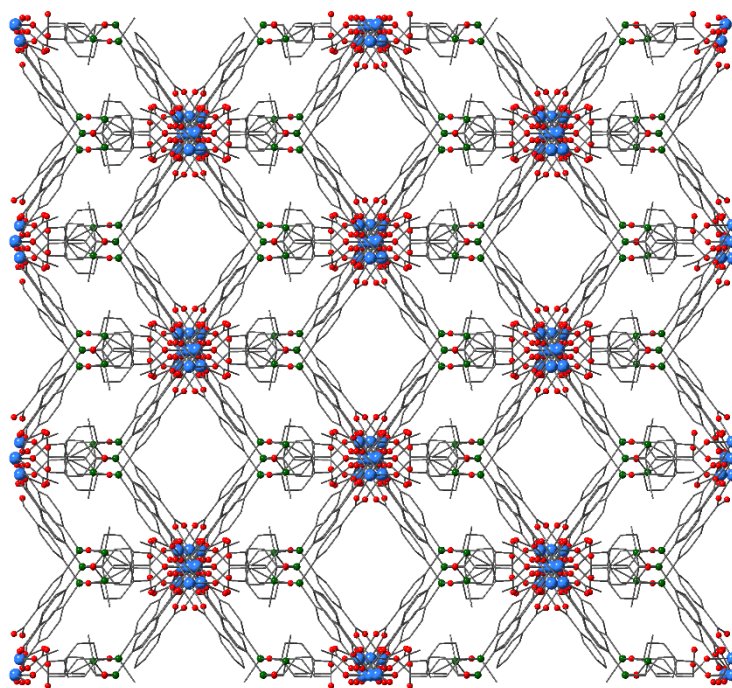


Figure S10: View of a portion of the **IMP-21** network along the [101] direction. Disorder, solvent molecules and hydrogen atoms omitted for clarity. Colour scheme: Zn, blue; O, red; C, grey; Si, green.

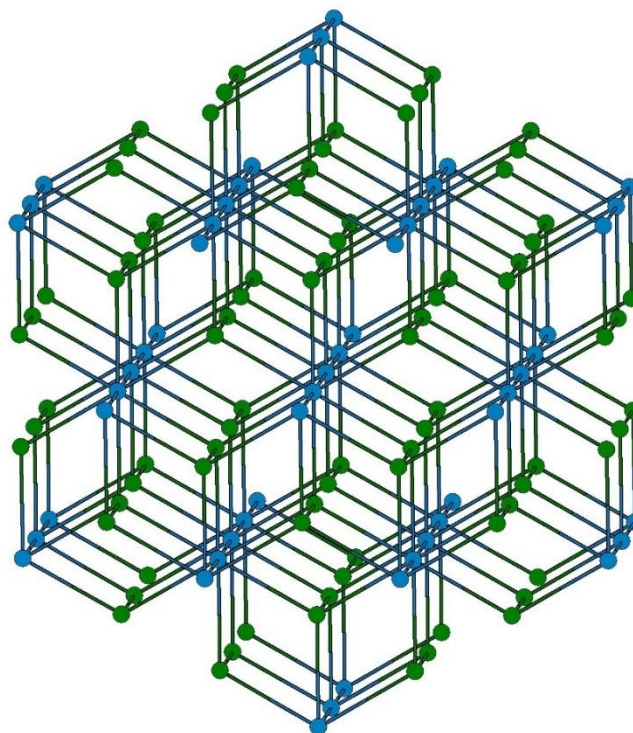


Figure S11: Topological view of **IMP-21** when **L** is considered as conjoined two tetrahedral nodes (shown in green) and Zn nodes as 8-connected (shown in blue) with bridging acetate groups acting as linear links between metal SBUs. Structure has been optimised using Systre¹⁰ such that the ideal symmetry of the crystal net has been assumed. This topology [whose point symbol is $\{4^{12} \cdot 6^{12} \cdot 8^4\}\{4^6\}_2$] has not been previously reported to the best of our knowledge.

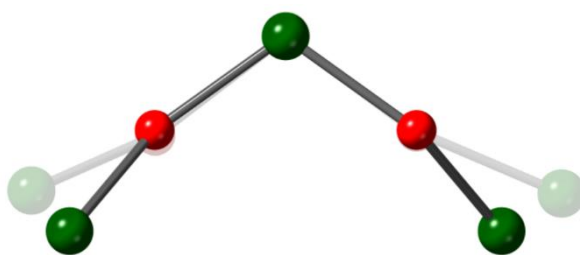


Figure S12: Overlay of the Si-O-Si-O-Si backbones of the **L** ligands showing the wider U-shaped conformation of **L** in **IMP-21** (background, faded) compared with the geometry of the **L** backbone in **IMP-22** (foreground) highlighting the overall flexibility of the trisiloxane unit. Colour scheme: O, red; C, grey; Si, green.

Table S1: Crystal data, data collection parameters and refinement parameters for **L**·H₆·AcOH·½H₂O, **IMP-20** and **IMP-21**. CCDC deposition numbers are 1836630, 1836631 and 1836632 respectively.

<i>Data</i>	L ·H ₆ ·AcOH·½H ₂ O	IMP-20	IMP-21
Formula	C ₄₆ H ₄₁ O _{16.5} Si ₃	C ₅₆ H ₅₈ N ₄ O ₁₈ Si ₃ Mn ₃	[C ₄₆ H ₃₃ O ₁₆ Si ₃ Zn ₃][C ₂ H ₈ N]
Solvent	-	6(C ₃ H ₇ NO)	3.75(C ₃ H ₇ NO)
Formula Weight	942.06	1762.72	1442.30
Color, habit	colourless blocks	colourless cones	colourless needles
Crystal size / mm ³	0.22 × 0.13 × 0.06	0.36 × 0.07 × 0.07	0.20 × 0.04 × 0.01
Temperature / K	173.00(14)	100(2)	100(2)
Crystal system	Monoclinic	Monoclinic	Monoclinic
Space group	<i>P2/n</i>	<i>C2/c</i>	<i>C2/c</i>
<i>a</i> / Å	15.1118(4)	18.9725(6)	32.1888(9)
<i>b</i> / Å	15.4367(5)	19.7061(5)	13.9804(3)
<i>c</i> / Å	40.6572(13)	25.3721(5)	30.8839(8)
α / deg	90	90	90
β / deg	95.516(3)	98.476(2)	95.684(3)
γ / deg	90	90	90
<i>V</i> / Å ³	9440.4(5)	9382.4(4)	13829.8(6)
<i>Z</i>	8	4	8
<i>D_c</i> / (g cm ⁻³)	1.326	1.248	1.385
Radiation used	Cu K α	Mo K α	Cu K α
μ / mm ⁻¹	1.533	0.506	2.312
2 θ max / deg	132	54	136
No. of unique reflections			
measured	16505	10752	12625
observed $ F_o > 4\sigma(F_o)$	12216	7396	10298
No. of variables	1197	794	633
<i>R</i> ₁ (obs), <i>wR</i> ₂ (all)	0.0761, 0.2439	0.0833, 0.2836	0.0471, 0.1406

References

1. H. E. Gottlieb, V. Kotlyar and A. Nudelman, *J. Org. Chem.*, 1997, **62**, 7512-7515.
2. G. Sheldrick, *Acta Crystallographica Section C*, 2015, **71**, 3-8.
3. G. Sheldrick, *Acta Crystallogr. Sect. A: Found. Crystallogr.*, 2015, **71**, 3-8.
4. O. V. Dolomanov, L. J. Bourhis, R. J. Gildea, J. A. K. Howard and H. Puschmann, *J. Appl. Crystallogr.*, 2009, **42**, 339-341.
5. L. Farrugia, *J. Appl. Crystallogr.*, 2012, **45**, 849-854.
6. A. L. Spek, *J. Appl. Crystallogr.*, 2003, **36**, 7-13.
7. D. Palmer, *CrystalMaker X for Win64 V10.1.1*, CrystalMaker Software Limited, Oxfordshire, England, 2009.
8. M. Wander, P. J. C. Hausoul, L. A. J. M. Sliedregt, B. J. van Steen, G. van Koten and R. J. M. Klein Gebbink, *Organometallics*, 2009, **28**, 4406-4415.
9. R. P. Davies, R. J. Less, P. D. Lickiss, K. Robertson and A. J. P. White, *Inorg. Chem.*, 2008, **47**, 9958-9964.
10. O. Delgado-Friedrichs and M. O'Keeffe, *Acta Crystallogr. Sect. A: Found. Crystallogr.*, 2003, **59**, 351-360.
11. Z. Liu, L. Lv, Y. He and Y. Feng, *CrystEngComm*, 2017, **19**, 2795-2801.
12. A. Karmakar, A. V. Desai and S. K. Ghosh, *Coord. Chem. Rev.*, 2016, **307**, 313-341.
13. J. Jiao, H. Liu, F. Chen, D. Bai, S. Xiong and Y. He, *Inorg. Chem. Front.*, 2016, **3**, 1411-1418.
14. R. P. Davies, R. Less, P. D. Lickiss, K. Robertson and A. J. P. White, *Cryst. Growth Des.*, 2010, **10**, 4571-4581.